Chapter 3
The Geometric Basis of Spatial Complexity

Classifying geometrical objects by their degrees of symmetry represents a sharp departure from the traditional classification of geometrical figures by their essences
(*Manuel De Landa* 2002, *p. 17*)

Abstract Spatial complexity emerges even from simple geometric objects, once they are arranged at non-trivial geometric positions. The geometric context of spatial complexity depends on the presence (or absence) of symmetries, orthogonality, number of intersections and geometry type (Euclidean or other). A simple spatial relationship (i.e. orthogonality of two sides of the triangle) makes the calculation of various geometric features (i.e. area, volume) less demanding in terms of operations required and hence, computation time and resources. Thus, key spatial details such as the relative position of two or more geometric objects and their intersections (regardless of their sizes) result in substantial differences in spatial complexity. Beyond these, research in polyominoes has furnished various computational complexity results, that are useful for the analysis of spatial complexity on squared surfaces.

Keywords Spatial complexity · Combinatorial complexity · Geocomputation · Coputational Geometry and Complexity · Polyominoes · Map Complexity

3.1 Orthogonality

Inequality is the cause of anomalies in nature
Thus we have gone through the origin of inequality
"Αἰτία δὲ ἀνισότης αὖ τῆς ἀνωμάλου φύσεως
ἀνισότητος δὲ γένεσιν μὲν διεληλύθαμεν"
(Plato, 428–348 b.C., "Timaeus", 58a)

In fact, even the tiniest spatial differences matter a lot for spatial complexity. In landscape analysis this has been examined before (Papadimitriou 2002), but to see why this is so, consider the calculation of the area of the simplest 2d spatial shape (the triangle) from the lengths of its sides: it is much simpler to calculate the area

F. Papadimitriou, *Spatial Complexity*, https://doi.org/10.1007/978-3-030-59671-2_3

of a right triangle with side lengths measured as *a*, *b* and *c*, than that of a scalene triangle. As known from high school, the area of a right triangle is calculated from Pythagoras' rule: *ab*/2, but the area of the scalene triangle is calculated from Heron's rule:

$$\sqrt{\left(\left(\frac{a+b+c}{2}\right)\left(\frac{a+b+c}{2}-a\right)\left(\frac{a+b+c}{2}-b\right)\left(\frac{a+b+c}{2}-c\right)\right)} \quad (3.1)$$

or (most often expressed in an abbreviated form) as:

$$\sqrt{\tau(\tau-a)(\tau-b)(\tau-c)}, \text{ where } \tau = (\alpha + \mathrm{b} + \mathrm{c})/2 \quad (3.2)$$

A simple spatial relationship (orthogonality of two sides of the triangle) therefore makes the calculation significantly less consuming in terms of computation time and resources. Thus key spatial details, such as the *relative position* of two or more geometric objects regardless of their sizes, result in substantial differences in spatial complexity. To verify this, one need only consider the algorithmic side of this calculation. A simple measure of complexity can be the number of arithmetic operations required to measure the area included within each triangle. The algorithm calculating a right triangle's area consists in *two* algebraic operations only (one multiplication followed by one division), but the algorithm for the calculation of the area of a scalene triangle requires as many as *ten* such operations (two additions, one division, three subtractions, three multiplications and one square root). One might be tempted to consider that calculating the area of a scalene triangle is more computationally expansive, because it is more "irregular" than that of a right triangle. This is true, but how much more irregular is it? Slightly so. In fact, only two of the three lines defining each triangle have a special relative position (a right angle) but precisely this special geometric relationship suffices to make a significant difference in the algorithmic process of the calculation of the area defined by each triangle: differences in geometric properties therefore imply differences in algorithmic procedures.

"*Small*" *but key spatial details may be responsible for significant differences in spatial complexity*: the calculation of the area of any scalene triangle is always more complex than that of a right triangle. And this is not because of the triangles' particular sizes, locations or orientations in space: it is a general property that applies to all triangles, however large or small they may be and whatever Euclidean space they may be embedded in: calculating the area of the tiniest scalene triangle will always be more computationally expansive than that of the hugest right triangle.

Expectedly, as the geometry of a surface changes, the calculation of spatial complexity may become more demanding. Indeed, the calculation of the area *A* of a spherical triangle with sides *a*, *b*, *c* is possible from a variant of Heron's formula for planar triangles as follows:

$$\tan\left(\frac{A}{4}\right) = \sqrt{\sin p \sin(p-a)\sin(p-b)\sin(p-c)}, \quad (3.3)$$

where $p = (a + b + c)/2$.

Hence, in the case of the spherical triangle, there are more complex operations to be made compared with the planar triangle and the calculation of the area of a planar triangle, however large it is, is always easier compared with that of a spherical triangle, however small that is. Changes in geometry therefore induce changes in spatial complexity.

3.2 Intersections

5. A surface is what has only length and breadth.

6. The extremities of a surface are lines.

"ε΄. Ἐπιφάνεια δέ ἐστιν, ὃ μῆκος καὶ πλάτος μόνον ἔχει.

ς΄. Ἐπιφανείας δὲ πέρατα γραμμαί".

(Euclid, fourth century b.C.,"Elements", Book A)

Let us now consider another example, showing how simple geometric elements can generate spatial complexity. We know that L lines on the plane intersect at $p_{\max}$ points:

$$p_{\max} = \frac{L(L-1)}{2} \tag{3.4}$$

Notice that this is *not* the number of intersection points generated by L lines in all cases. Specifically, the number u of possible intersections can be calculated from the formula

$$u_{L,k} = \binom{L}{k} \tag{3.5}$$

with k lines intersecting the other L-k lines.

For instance, if there are $L = 3$ lines, then the cases that $k = 0,1,2,3$ lines intersect with the remaining L-k lines are given in Fig. 3.1 and if, i.e. there are only one line ($k = 1$) intersecting the remaining L-$k = 2$ lines, then there are three cases of intersection:

$$u_{3,1} = \binom{3}{1} = \frac{3!}{2!} = 3 \tag{3.6}$$

In exactly the same way, if $L = 4$ and $k = 2$, then the number is (Fig. 3.2):

$$u_{4,2} = \binom{4}{2} = \frac{4!}{2!2!} = 6 \tag{3.7}$$

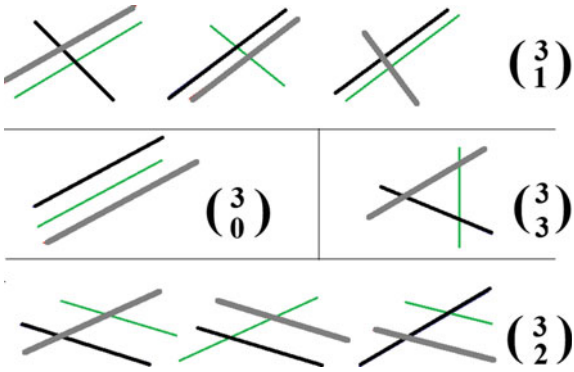

Fig. 3.1 Number of cases of intersections for $L = 3$ lines, when $k = 0$, or $k = 1$, $k = 2$ or $k = 3$ of them intersect the remaining L-k lines

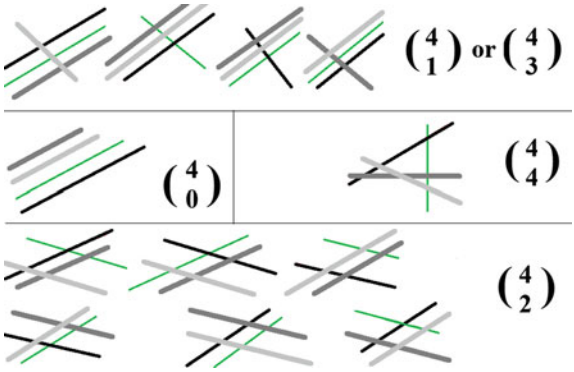

Fig. 3.2 Alternative cases of intersection of $L = 4$ different lines, when $k = 0$, 1, 2, 3, 4

Notice that the number of intersection points $p_{\max}$ result in only one case:

$$u_{L,L} = \binom{L}{L} = 1 \tag{3.8}$$

Proceeding from lines to areas, we may observe that intersecting lines define intersecting areas on the plane. Beginning with $L = 2$ lines, observe that these define one intersection point. Continuing with more lines i.e. up to $L = 7$ (as shown in Fig. 3.3), then progressively more areas are defined in between the intersecting lines and the maximum number of possible such areas is given by the formula:

$$A_{\max} = \frac{(L-1)(L-2)}{2}. \tag{3.9}$$

Now a natural question to ask is how the ratios among lines, intersection points and areas grow with increasing number of lines (L). The answer essentially lies in calculating the following limits:

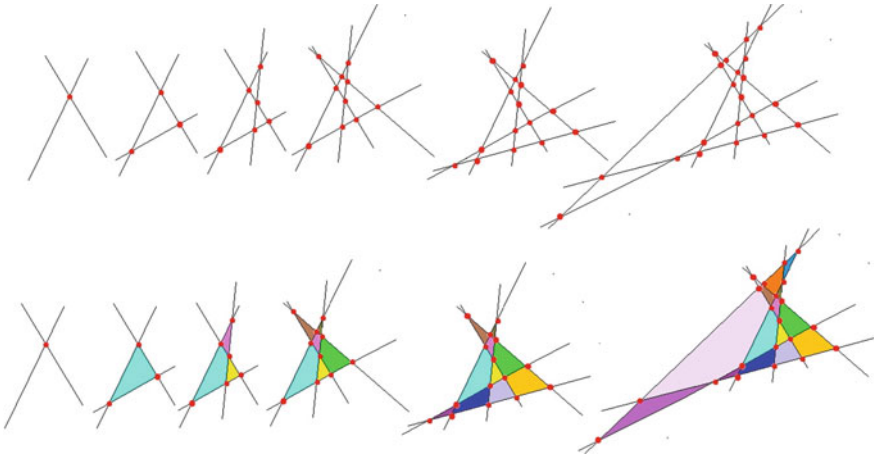

Fig. 3.3 Maximum intersection points ($p_{\max}$) defined by 2 to 7 intersecting straight lines (up, from left to right) and regions ($a_{\max}$) defined by these maximum intersection points (bottom, from left to right)

$$\lim_{L\to\infty} \frac{A_{\max}}{p_{\max}} = \lim_{L\to\infty} \left(1 - \frac{2}{L}\right) = 1 \tag{3.10}$$

$$\lim_{L\to\infty} \frac{p_{\max}}{L} = \lim_{L\to\infty} \left(\frac{L}{2} - \frac{1}{2}\right) = \infty \tag{3.11}$$

$$\lim_{L\to\infty} \frac{A_{\max}}{L} = \lim_{L\to\infty} \left(\frac{L}{2} - \frac{3}{2} + \frac{1}{L}\right) = \infty \tag{3.12}$$

Thus, as the number of lines tends to infinity, the number of intersection points approximates the number of areas defined in-between lines. While the complexity of calculating the maximum number of intersection points is polynomial (a function of L^2), the number of areas generated tend to infinity with respect to the number of intersecting lines. This means that as more intersecting lines are drawn on the plane, a lot more areas can be defined by their possible intersections. Otherwise stated, the more 1d objects are used to shape 2d spaces, the more such 2d spaces emerge. The previous formula was for the definition of areas only inside the intersections. If areas outside the intersection regions are also considered, then the formula giving the number of regions A is (Fig. 3.4):

$$A_{\max} = \binom{L+1}{2} + 1 \tag{3.13}$$

Thus, spatial complexity can be created by simple geometric objects, once they are arranged at non-trivial geometric positions.

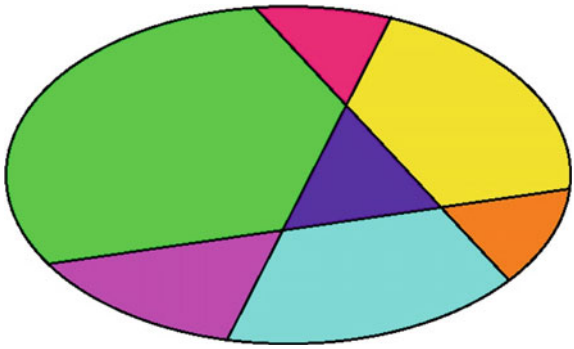

Fig. 3.4 The maximum number of areas A defined by L lines both inside and outside the lines' intersections. In this case, $L = 3$, so there are $A = 7$ regions

3.3 Curvature and Non-Euclidean Geometries

"On Red Square the earth is roundest,
its slope more firm,
on Red Square the earth is roundest,
and its slope suddenly undolds"
(Osip Mandelstam,1891–1938,"Children's Haircut", 1935)

Curvature has been considered as a determinant of complexity for curves and curved surfaces (Ujiie et al. 2012; Matsumoto et al. 2019). Among all formulas of geometry, the "isoperimetric inequality" is probably the more appropriate one to describe the degree of complexity of a shape C that is circumscribed by a curve $\gamma(t) = (x(t),y(t))$:

$$L^2 \geq 4\pi A \tag{3.14}$$

where L is the curve length and A is the area defined by the curve γ:

$$A = \oint_C F(x, y) \cdot d\gamma = \int_{\alpha}^{\beta} x(t)y'(t)dt \tag{3.15}$$

It is easy to verify that when the shape is a circle, then $L^2 = 4\pi A$ and, hence, the ratio:

$$L^2/4\pi \mathrm{A} \tag{3.16}$$

is a geometric assessor of the complexity of a 2d-shape: the higher the ratio, the more complex the shape is (Fig. 3.5).

The mean curvature of a surface is an old problem in geometry, which consists in seeking the surface of the largest area among all compact surfaces in the Euclidean

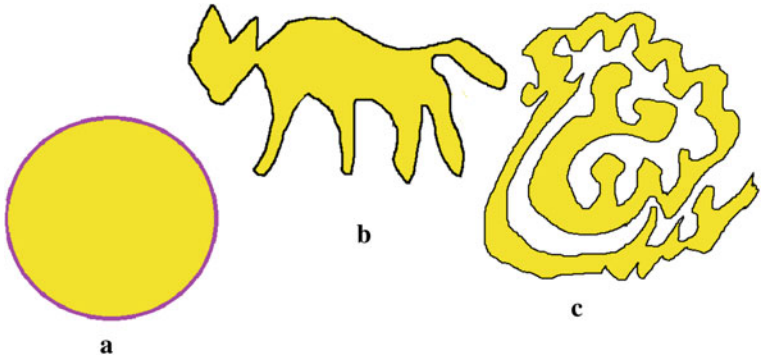

Fig. 3.5 Using the isoperimetric inequality to assess spatial complexity: Among shapes with the same area, but with different perimeter lengths, more spatially complex is the one with the higher perimeter length (**c** is more spatially complex than **b**, and **b** more complex than **a**)

space enclosing a fixed volume. The obvious solution to this problem is the sphere. But keeping the geometric properties as elementarily simple as those of a triangle and changing the geometry type induces considerable changes in spatial complexity.

In assessing the impact of curvature on spatial complexity, one needs to recall that the Gaussian curvature K_G of a surface is calculated on the basis of the three variables (E_C, F_C, G_C) of the "first fundamental form", which, as known from differential geometry, is equal to

$$E_C du^2 + 2F_C du dv + G_C dv^2 \tag{3.17}$$

leading to the well known (and cumbersome) formula:

$$K_G = \frac{\begin{vmatrix} -\frac{1}{2}E_{vv} + F_{uv} - \frac{1}{2}G_{uu} & \frac{1}{2}E_u & F_u - \frac{1}{2}E_v \\ F_v - \frac{1}{2}G_u & E_C & F_C \\ \frac{1}{2}G_v & F_C & G_C \end{vmatrix} - \begin{vmatrix} 0 & \frac{1}{2}E_v & \frac{1}{2}G_u \\ \frac{1}{2}E_v & E_C & F_c \\ \frac{1}{2}G_u & F_C & G_C \end{vmatrix}}{\sqrt{E_C G_C - F_C^2}} \tag{3.18}$$

As a result of Gauss's "Theorema Egregium", there is no planar map representing the curved surface of the earth, without distorting distances. This is because this theorem guarantees that Gaussian curvature K_G must be the same so long as there are local isometries. As the surface of a sphere has a non-zero curvature and the planar map has zero curvature, the respective K_G curvatures are different, and therefore there are no local isometries. Thus, curved surfaces generate objects of higher spatial complexity since they require more calculations to measure lengths and areas. The effect of curvature becomes more decisive for spatial complexity in the case of non-Euclidean geometries. In the case of Euclidean geometry, the length of the curve connecting points x and y is:

$$L = \int |\frac{dx(t)}{dt}|dt \tag{3.19}$$

but in a hyperbolic geometry, the distance is:

$$L = \int \frac{1}{1 - \frac{1}{4}|x(t)|^2} |\frac{dx(t)}{dt}|dt \tag{3.20}$$

so the computation of length in cases of non-euclidean geometries involves more calculations.

Increasing complexity by mounting dimension from two to three further increases the spatial complexity of a shape. Take, for instance, the calculation of the volume of a spherical tetrahedron. This is tantamount to changing the geometry to spherical and adds up more complexity to the calculations. It may come as a surprise that there is no simple formula available for the spherical tetrahedron. In fact, the volume of an arbitrary tetrahedron in a space of nonzero curvature was first calculated only shortly before the beginning of this century (Cho and Kim 1999) for spaces of hyperbolic curvature. This was later also calculated by means of other formulas (Murakami and Ushijima 2005; Murakami and Yano 2005) for the same type of curvature. Murakami (2011) obtained a formula for the volume of the spherical tetrahedron. This is given here without detailed explanation; simply for the sake of illustration of how a lot more complex the calculation of volumes gets when it extends to geometries of non-zero curvature:

$$\begin{aligned} V = & \operatorname{Re}\Big(\tilde{L}(b_1, b_{2,}, \ldots, b_6, \tilde{z}_0)\Big) - \pi \arg(-\tilde{q}_2) \\ & - \sum_{j=1}^{6} \frac{\partial \operatorname{Re}\Big(\tilde{L}(b_1, b_{2,}, \ldots, b_6, z)\Big)}{\partial l_j} |_{z=\tilde{z}_0} - \frac{\pi^2 \bmod (2\pi^2)}{2} \end{aligned} \tag{3.21}$$

Notice that, if not anything else, this calculation can not be effectuated without using complex numbers and the dilogarithm function.

3.4 Spatial Combinatorics and Polyominoes

Precise ideas often lead to doing nothing
"Les idées précises conduisent souvent à ne rien faire"
(Paul Valéry, 1871–1945, Mélange, 1934)

Spatial complexity also emerges from geometric combinatorics. Enumerating possible compositions of square cells resulting from geometric arrangements of simple geometric objects is a straightforward method to evaluate the combinatorial complexity of spatial patterns.

The "map coloring" problem consists in the determination of the least number of colors to color any map. In 2d, the "*Four colors problem*" was to prove that any map can be colored with no more than 4 colors, whatever the spatial arrangement of the regions shown on it. After perplexing too many people, it was solved in 1976 by K. Appel and W. Haken. A generalization was achieved with the *Colin de Verdiere number* μ(G), which is an invariant for a graph G (Colin de Verdiere 1990) and any graph with a CdV invariant μ may be colored with at most $\mu + 1$ colors. Planar graphs have $\mu = 3$ and, by means of the "Four Color Theorem" can be colored by at most $\mu + 1 = 4$ colors. Disjoint unions of paths ("linear forests") have $\mu = 1$ and therefore can be colored by at most 2 colors. Thus four colours are enough to color any map, with the exception of some exceptionally complex cases (one example of which is the "*Wada lakes*", that is regions sharing the same boundary). In the case of Wada lakes, the number of colors required is as number as the number of regions defined by the "lakes". In some sense therefore, the minimum number of colors necessary to color just *any* map remains an unsolved problem.

Aside of the colors problem, an example of combinatorial complexity emerging from spatial problems is the problem of covering the plane with polyominoes. A polyomino is a plane geometric shape formed by joining one or more squares of equal area, edge to edge (Fig. 3.6) and is classified according to how many square cells it consists in (with 2-cells it is called "domino", with three cells "triomino", with 4 cells "tetromino" and so on).

Several interesting results relate to tiling squares with polyominoes. For instance, it is known that square maps can (or can not) be tiled by n-ominoes depending on whether they are even–numbered or odd-numbered, i.e. a 7×7 square map can not be tiled by dominoes (Fig. 3.7).

The complexity of spatial arrangements of polyominoes is interesting because several problems involving them are intractable. It suffices to observe that the number of polyominoes with n cells increases fast, giving a glimpse of the high combinatorial complexity involved: 1, 2, 5, 12, 35, 108, 369, 1285, 4655, 17,073, 63,600, 238,591, 901,971, 3,426,576, 13,079,255, 50,107,909… (corresponding to the Sloane sequence A000105). But high combinatorial complexity in spatial

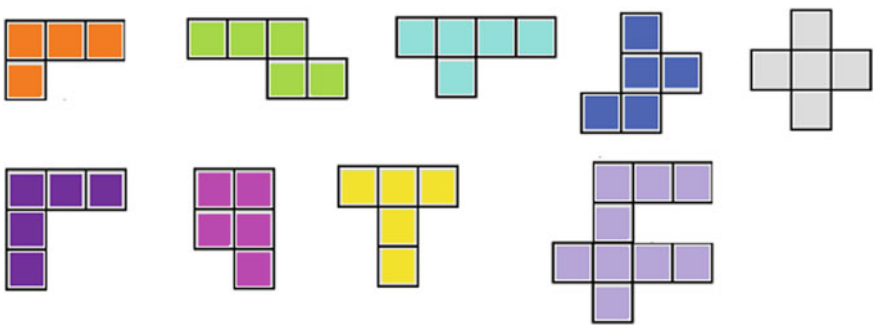

Fig. 3.6 Polyominoes of various sizes

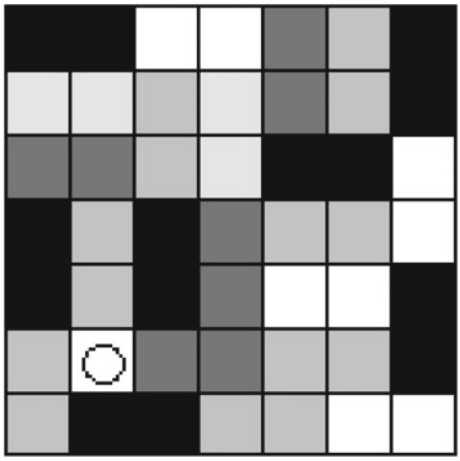

Fig. 3.7 Odd-numbered square maps (7 × 7 here) can *not* be tiled by dominoes

arrangements may emerge even from much simpler cases, i.e. when trying to practically solve simple spatial combinatorial problems.

In this respect, there already are some interesting results about combinations of particular types of 3d polyominoes (Fig. 3.8). In two dimensions, we know that a *m*x*n* rectangle can be tiled with O-tetrominoes, if and only if m and n are even, if a $n \times n$ square can be tiled with T-tetrominoes, then n^2 is divisible by 8, a $n \times n$ square can be tiled with L-trominoes with fourfold rotational symmetry if and only if n is divisible by 6, a $n \times n$ square can be tiled with L-tetrominoes with fourfold

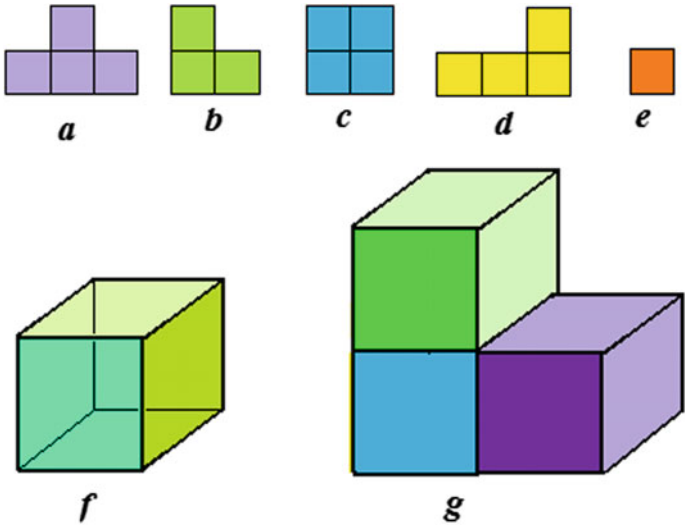

Fig. 3.8 Some types of 2d-and-3d-polyominoes: T-tetromino (**a**), L-tromino (**b**), O-tetromino (**c**), L-tetromino (**d**), Monomino (**e**), 3d monomino (**f**) and 3d L-tromino (**g**)

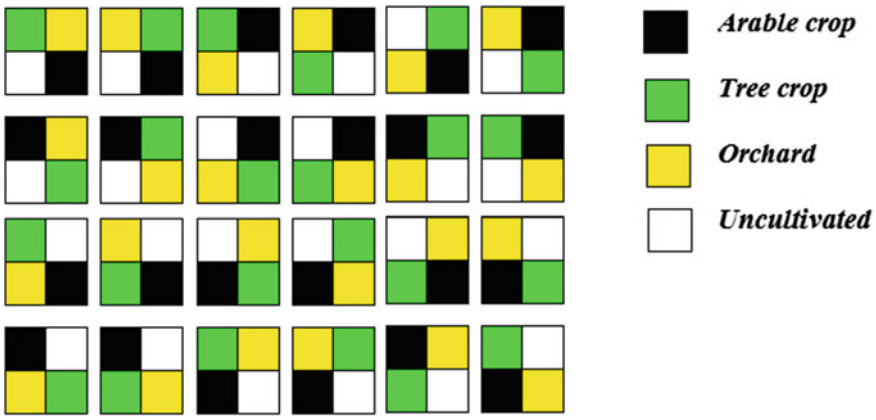

Fig. 3.9 A solution to the spatial combinatorial problem (see text for explanation): there are 24 alternative land cultivation schemes if one of the four pieces of land is left uncultivated (too many spatial alternative configurations to decide, even for such a simple problem)

rotational symmetry if and only if n is divisible by 4 and any $2^n \times 2^n$ square can be tiled by a monomino and trominoes (Golomb 1954; 1996).

Equivalently, there are similar (unfortunately fewer) results for polyominoes in 3d: any $2^n \times 2^n \times 2^n$ cube with $n = 1(\text{mod}3)$ can be tiled with a 3d monomino and 3d L-trominoes (Starr, 2008) and a mxnxk parallelepiped can be packed with 3d L-trominoes if and only if mnk is divisible by 3 (Soifer 2010).

Spatial combinatorial problems are well known for producing big numbers quickly. Consider, for instance, the following spatial planning problem:

A farmer owns a square lot of side length x, which can be divided in four equal squares, of side length $x/2$ each. He has three types of cultivations to allocate on these four squares: arable crops, tree crops and orchards. How many alternative land cultivation schemes are there for the three crop types on the four squares pieces of land, provided that all three cultivations types should be used in that lot? The farmer also needs to know the possible spatial arrangements if one quarter of the land is left uncultivated each time.

There are 24 alternative land cultivation schemes if one of the four squares is left uncultivated (Fig. 3.9), and as many as 36 different land cultivation schemes if all squares are occupied by cultivations. Even in this simple land allocation scheme of only 4 spatial regions and 3 types of spatial entities, it is evident that the number of possible combinations becomes rapidly high; may be unacceptably high for ordinary (i.e. everyday) spatial decision-making.

References

Cho, Y., & Kim, H. (1999). On the volume formula for hyperbolic tetrahedra. *Discrete Computational Geometry, 22*(3), 347–366.

Colin de Verdière, Y. (1990). Sur un nouvel invariant des graphes et un critère de planarité. *Journal of Combinatorial Theory B, 50*(1), 11–21.

De Landa, M. (2002). *Intensive Science and Virtual Philosophy*. London: Continuum.

Golomb, S. W. (1954). Checker boards and polyominoes. *American Mathematical Monthly, 61,* 675–682.

Golomb, S. W. (1996). *Polyominoes: Puzzles, Patterns, Problems, and Packings*. Princeton NJ: Princeton University Press.

Matsumoto, T., Sato, K., Matsuoka, Y., & Kato, T. (2019). Quantification of "complexity" in curved surface shape using total absolute curvature. *Computers and Graphics, 78,* 108–115.

Murakami, J. (2011). Volume formulas for a spherical tetrahedron. arXiv:1011.2584v4 [math.MG] 2 May 2011.

Murakami, J., & Ushijima, A. (2005). A volume formula for hyperbolic tetrahedra in terms of edge lengths. *Journal of Geometry, 83,* 153–163.

Murakami, J., & Yano, M. (2005). On the volume of a hyperbolic and spherical tetrahedron. *Communications in Analytic Geometry, 13,* 379–400.

Papadimitriou, F. (2002). Modelling indicators and indices of landscape complexity: An approach using GIS. *Ecological Indicators, 2,* 17–25.

Soifer, A. (2010). *Geometric Etudes in Combinatorial Mathematics.* New York: Springer.

Starr, N. (2008). Tromino tiling deficient cubes of side length 2*n*. *Geombinatorics, XVIII, 2,* 72–87.

Ujiie, Y., Kato, T., Sato, K., & Matsuoka, Y. (2012). Curvature entropy for curved profile generation. *Entropy, 14,* 533–558.